Contents lists available at ScienceDirect

Biochemical Pharmacology

journal homepage: www.elsevier.com

Potent inhibitors of human LAT1 (SLC7A5) transporter based on dithiazole and dithiazine compounds for development of anticancer drugs

Lara Napolitano[a, 1], Mariafrancesca Scalise[a, 1], Maria Koyioni[b], Panayotis Koutentis[b], Marco Catto[c], Ivano Eberini[d], Chiara Parravicini[d], Luca Palazzolo[e], Leonardo Pisani[c], Michele Galluccio[a], Lara Console[a], Angelo Carotti[c], Cesare Indiveri[a, *]

[a] *Department DiBEST (Biologia, Ecologia, Scienze della Terra) Unit of Biochemistry and Molecular Biotechnology, University of Calabria, Via P. Bucci 4C, 87036 Arcavacata di Rende, Italy*
[b] *Department of Chemistry, University of Cyprus, P.O. Box 20537, 1678 Nicosia, Cyprus*
[c] *Dipartimento Farmaco-Chimico, Università degli Studi "Aldo Moro", via Orabona 4, 70125 Bari, Italy*
[d] *Dipartimento di Scienze Farmacologiche e Biomolecolari, Università degli Studi di Milano, Italy*
[e] *Dipartimento di Scienze Farmacologiche e Biomolecolari e Dipartimento di Scienze Biomediche e Cliniche "L. Sacco", Università degli Studi di Milano, Italy*

ARTICLE INFO

Article history:
Received 17 May 2017
Accepted 7 July 2017
Available online xxx

Keywords:
LAT1 inhibitors
1,2,3-Dithiazoles
1,2,4-Dithiazines
Mechanism of inhibition
Pharmacological target
Cancer

ABSTRACT

The LAT1 transporter is acknowledged as a pharmacological target of tumours since it is strongly overexpressed in many human cancers. The purpose of this work was to find novel compounds exhibiting potent and prolonged inhibition of the transporter. To this aim, compounds based on dithiazole and dithiazine scaffold have been screened in the proteoliposome experimental model. Inhibition was tested on the antiport catalysed by hLAT1 as transport of extraliposomal [^{3}H]histidine in exchange with intraliposomal histidine. Out of 59 compounds tested, 8 compounds, showing an inhibition higher than 90% at 100 μM concentration, were subjected to dose-response analysis. Two of them exhibited IC_{50} lower than 1 μM. Inhibition kinetics, performed on the two best inhibitors, indicated a mixed type of inhibition with respect to the substrate. Furthermore, inhibition of the transporter was still present after removal of the compounds from the reaction mixture, but was reversed on addition of dithioerythritol, a S-S reducing agent, indicating the formation of disulfide(s) between the compounds and the protein. Molecular docking of the two best inhibitors on the hLAT1 homology structural model, highlighted interaction with the substrate binding site and formation of a covalent bond with the residue C407. Indeed, the inhibition was impaired in the hLAT1 mutant C407A confirming the involvement of that Cys residue. Treatment of SiHa cells expressing hLAT1 at relatively high level, with the two most potent inhibitors led to cell death which was not observed after treatment with a compound exhibiting very poor inhibitory effect.

1. Introduction

LAT1 (SLC7A5) is a transporter belonging to the Heterodimeric Amino acid Transporters group (HATs). In particular, LAT1 represents the light chain associated with the glycoprotein CD98 (SLC3A2) via a disulfide between two conserved cysteine residues [1]. The heterodimer is mainly expressed at the plasma membrane; however, its presence in lysosomal membrane has also been reported [2].

The biomedical and pharmacological interest on LAT1 lies on its over-expression in many tumors [3]. Based on its specificity for branched chain amino acids and for Gln, it is involved in "Glutamine addiction", a typical feature of tumor cells that use Gln for energy purpose at a much higher rate than normal ones. In these cells, LAT1 realizes a Gln/Leu cycle together with another transporter, ASCT2, that is a Na^+-dependent antiporter for Gln and other neutral amino acids. Therefore, both transporters are involved in cancer growth and progression [4]. LAT1 is, indeed, considered as a marker of malignancy [3,5,6] and as a new pharmacological target [7,8]. Several research groups worldwide are involved in discovering new compounds able to inhibit LAT1 mediated transport. The most common approaches used to achieve this goal are: i) *in silico* virtual screening that, however, requires high quality three dimensional structure of the target (not available for LAT1) and ii) *in vitro* screening, generally performed with cell models. Recently, we exploited proteoliposome technology for assaying LAT1 function. This model allows the detection of transport activity in absence of interferences by other transporters or enzymes. The purpose of this work was to identify novel

Abbreviations: LAT, L-type amino acid transporters 1; SLC, solute carrier; CD98, cluster of differentiation 98; ASCT2, AlaSerCys Transporter 2; mTOR, mammalian target of rapamycin; BBB, blood brain barrier; AdiC, L-arginine/agmatine antiporter; $C_{12}E_8$, octaethylene glycol monododecyl ether; BCH, 2-amino-2-norbornanecarboxylic acid; DTE, dithioerythritol; TX-100, Triton X-100

* Corresponding author.
Email address: cesare.indiveri@unical.it (C. Indiveri)
[1] These authors contributed equally to this work.

http://dx.doi.org/10.1016/j.bcp.2017.07.006
0006-2952/

and more potent inhibitors than those so far described. To achieve this aim we exploited the structure/function relationships of this transporter, recently revealed [9]. LAT1 was demonstrated to be the sole transport competent subunit of the heterodimer, able to recognize His as one of the major substrates [9–11]. The physiological importance of this substrate was highlighted by the occurrence of Autism Spectrum Disorders in patients with inherited defects of LAT1 [10]. The structure of LAT1, differently from that of CD98 [12], is only predicted by homology modeling [9,13]. Therefore, some important structural features have been deciphered using bioinformatics and site-directed mutagenesis. The substrate binding site is characterized by the key residues F252, S342, C335 and C407 [9].

The presence of Cys residues in the active site was exploited to design molecules that might form disulfides leading to irreversible inhibition. Using proteoliposome technology, a large number of potential irreversible inhibitors with dithiazole- or dithiazine-based structures was screened. Interestingly, we recently reported dithiazoles as strong inhibitors of the rat isoform of ASCT2 by reacting with Cys residue(s) of the protein [14,15]. The results obtained in the present study led to the identification of the most potent hLAT1 inhibitors so far described.

2. Materials and methods

2.1. Materials

His Trap HP columns and PD-10 columns were purchased from GE Healthcare; radiolabeled amino acids were purchased from ARC (American Radiolabeled Chemicals); all the other reagents are from Sigma-Aldrich.

*2.2. Synthesis of 1,2,3-dithiazoles **1**–**55** and 1,2,4-dithiazines **56**–**59***

2.2.1. General methods and materials

Reactions were protected from atmospheric moisture by $CaCl_2$ drying tubes. Anhydrous Na_2SO_4 was used for drying organic extracts, and all volatiles were removed under reduced pressure. Decomposition points were determined using the TA Instrument DSC Q1000 with samples hermetically sealed in aluminium pans under an argon atmosphere, using heating rates of 5 °C/min. UV/vis spectra were obtained using a Shimadzu UV-1601 UV/vis spectrophotometer and inflections are identified by the abbreviation "inf". IR spectra were recorded on a Shimadzu FTIR-NIR Prestige-21 spectrometer with a Pike Miracle Ge ATR accessory. NMR spectra were recorded on a Bruker Avance 500 MHz instrument. Deuterated solvents were used for homonuclear lock and internal calibration. MALDI-TOF mass spectra were recorded on a Bruker Autoflex III Smartbeam instrument. Elemental analysis was performed on a Perkin Elmer 2400 Series Elemental Analyzer by Stephen Boyer of London Metropolitan University.

*2.2.2. Synthesis of 1,2,3-dithiazoles **1**–**55***

For the preparation of the 1,2,3-dithiazoles, primary aromatic or heteroaromatic amines or alcohols were reacted with 4,5-dichloro-1,2,3-dithiazolium chloride (Appel's salt) I, followed by treatment with base (2 equiv) to give the corresponding [(4-chloro-5*H*-1,2,3-dithiazol-5-ylidene)amino]arenes or 2-(4-chloro-5*H*-1,2,3-dithiazol-5-ylidene)arene-1(2*H*)-ones **1**–**53** in moderate to excellent yields [16–18] according to the following general procedure: to a stirred suspension of Appel's salt I (100 mg, 0.48 mmol) in dichloromethane (4 mL) at *ca.* 20 °C was added the corresponding aminoarene or hydroxyarene (0.48 mmol). After 1 h, the appropriate base [*e.g.* Hunig's base (167 µL, 0.96 mmol)] was added dropwise to the reaction mixture. After stirring of 2 h the reaction mixture was loaded onto silica and purified by dry flash chromatography to afford the corresponding [(4-chloro-5*H*-1,2,3-dithiazol-5-ylidene)amino]arene or 2-(4-chloro-5*H*-1,2,3-dithiazol-5-ylidene)arene-1(2*H*)-one (Fig. 1 A).

Analytical and spectroscopic data of the 1,2,3-dithiazoles **1**–**46** and **51**–**53** have been previously reported [14]. Analytical, physicochemical and spectroscopic data of the newly synthesized 1,2,3-dithiazoles **47**–**50** are reported below:

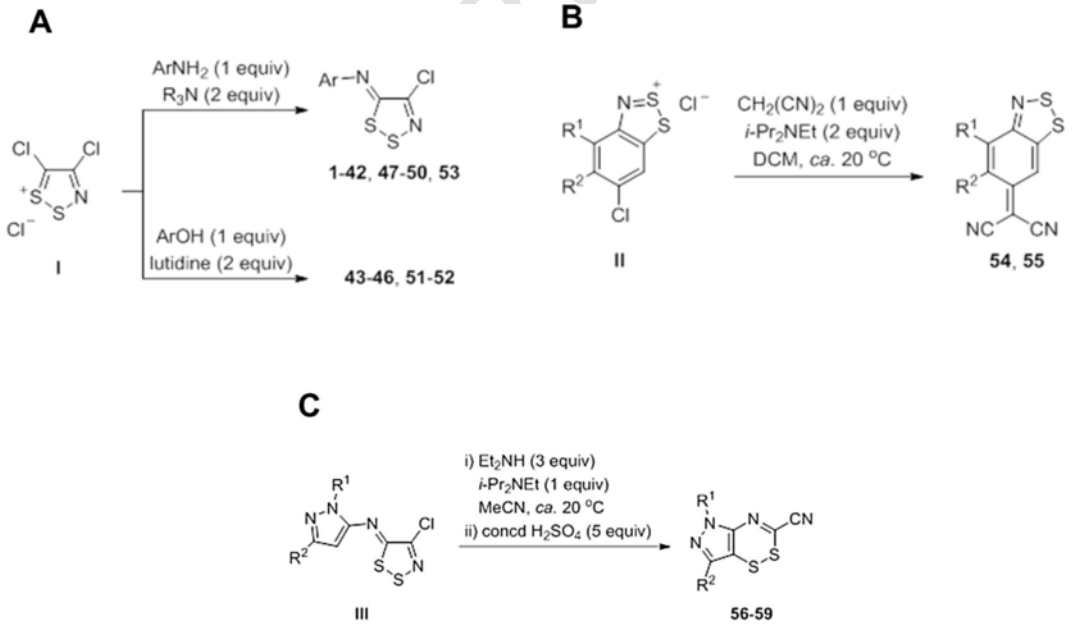

Fig. 1. Conditions for the synthesis of the compounds from **1** to **53** (A), **54**–**55** (B) or **56**–**59** (C).

*2.2.2.1. (Z)-4-Chloro-N-[4-(morpholinomethyl)phenyl]-5H-1,2,3-dithiazol-5-imine **(47)***

Yellow oil (66%); R_f 0.35 (DCM/Et_2O, 70:30); (found: C, 47.59; H, 4.38; N, 13.01. $C_{13}H_{14}ClN_3OS_2$ requires C, 47.62; H, 4.30; N, 12.82%); λ_{max}(DCM)/nm 240 inf (log ε 4.16), 305 (3.44), 378 (3.84), 387 inf (3.83), 410 inf (3.72); ν_{max}/cm^{-1} 2955w, 2853w and 2805m (alkyl C-H), 1582m, 1533w, 1497m, 1452m, 1414w, 1395w, 1368w, 1348m, 1333m, 1308w, 1292m, 1263m, 1221m, 1115s, 1069m, 1034m, 1007m, 914m, 866s, 797m, 764m; δ_H(500 MHz, acetone-d_6) 7.49 (1H, d, *J* 8.2), 7.23 (1H, d, *J* 8.4), 3.63 (2H, t, *J* 4.7), 3.55 (1H, s), 2.44 (3H, br s); δ_C(125 MHz, acetone-d_6) 158.8 (s), 150.9 (s), 148.7 (s), 137.3 (s), 131.4 (d), 120.4 (d), 67.4 (t), 63.3 (t), 54.4 (t); *m*/*z* (MALDI-TOF) 328 (M^++1, 41%), 326 (M^+−1, 100).

*2.2.2.2. (Z)-4-Chloro-N-[3-(morpholinomethyl)phenyl]-5H-1,2,3-dithiazol-5-imine **(48)***

Yellow oil (81%), decomp. (DSC) onset: 145.6 °C, peak max: 150.5 °C; R_f 0.48 (DCM/Et_2O, 70:30); (found: C, 47.70; H, 4.20; N, 12.94. $C_{13}H_{14}ClN_3OS_2$ requires C, 47.82; H, 4.30; N, 12.82%); λ_{max}(DCM)/nm 238 inf (log ε 4.11), 302 (3.35), 377 (3.78), 386 inf (3.77), 409 inf (3.63); ν_{max}/cm^{-1} 2957w, 2855w and 2805m (alkyl C-H), 1578m, 1524w, 1503w, 1479m, 1454m, 1433m, 1396w, 1368w, 1348m, 1331m, 1300m, 1281m, 1261m, 1206w, 1163m, 1115s, 1069m, 1034m, 1009m, 908m, 885m, 856s, 806m, 785m, 758m; δ_H(500 MHz, $CDCl_3$) 7.41 (1H, dd, *J* 7.7, 7.7), 7.26–7.15 (2H, m), 7.11 (1H, d, *J* 7.8), 3.71 (5H, t, *J* 4.5), 3.53 (2H, s), 2.46 (4H, br s); δ_C(125 MHz, $CDCl_3$) 158.6 (s), 151.2 (s), 147.9 (s), 140.0 (s), 129.7 (d), 127.3 (d), 120.0 (d), 118.1 (d), 67.0 (t), 63.1 (t), 53.6 (t); *m*/*z* (MALDI-TOF) 328 (MH^+, 36%), 326 (M^+−1, 100), 292 (2), 260 (23), 233 (6), 153 (3).

*2.2.2.3. (Z)-N-Benzyl-1-{3-[(4-chloro-5H-1,2,3-dithiazol-5-ylidene)amino]phenyl}-N-methylmethanamine **(49)***

Yellow oil (86%), decomp. (DSC) onset: 145.3 °C, peak max: 154.1 °C; R_f 0.47 (DCM/Et_2O, 90:10); (found: C, 56.49; H, 4.38; N, 11.73. $C_{17}H_{16}ClN_3S_2$ requires C, 56.42; H, 4.46; N, 11.61%); λ_{max}(DCM)/nm 241 inf (log ε 4.17), 316 inf (3.45), 378 (3.83), 388 inf (3.82), 409 inf (3.69); ν_{max}/cm^{-1} 3059w and 3026w (aryl C-H), 2833w and 2785m (alkyl C-H), 1578s, 1495m, 1479m, 1452m, 1415w, 1364m, 1250m, 1159m, 1132m, 1076w, 1026m, 988m, 951w, 934w, 905m, 887m, 856s, 787m, 760m; δ_H(500 MHz, $CDCl_3$) 7.41 (1H, dd, *J* 7.7, 7.7), 7.40–7.36 (2H, m), 7.33 (2H, dd, *J* 7.5, 7.5), 7.30–7.21 (3H, m), 7.11 (1H, d, *J* 8.0), 3.57 (2H, s), 3.56 (2H, s), 2.21 (2H, s); δ_C(125 MHz, $CDCl_3$) 158.5 (s), 151.2 (s), 148.0 (s), 141.4 (s), 138.9 (s), 129.7 (d), 128.9 (d), 128.3 (d), 127.1 (d), 127.0 (d), 119.7 (d), 118.0 (d), 61.9 (t), 61.4 (t), 42.2 (q); *m*/*z* (MALDI-TOF) 362 (MH^+, 31%), 360 (M^+−1, 100), 294 (17), 267 (18), 91 (1).

*2.2.2.4. (Z)-N-Benzyl-1-{4-[(4-chloro-5H-1,2,3-dithiazol-5-ylidene)amino]phenyl}-N-methylmethanamine **(50)***

Yellow oil (90%), decomp. (DSC) onset: 142.7 °C, peak max: 150.5 °C; R_f 0.36 (DCM/Et_2O, 70:30); (found: C, 56.35; H, 4.38; N, 11.50. $C_{17}H_{16}ClN_3S_2$ requires C, 56.42; H, 4.46; N, 11.61%); λ_{max}(DCM)/nm 242 inf (log ε 4.15), 301 (3.49), 388 (3.85), 410 inf (3.65); ν_{max}/cm^{-1} 3026w (aryl C-H), 2920w, 2837w and 2785m (alkyl C-H), 1582m, 1533w, 1497m, 1452m, 1410w, 1366m, 1342w, 1308w, 1292w, 1265w, 1236m, 1219m, 1171m, 1134m, 1099m, 1024m, 1013m, 901s, 860s, 799w, 764s; δ_H(500 MHz, acetone-d_6) 7.56 (2H, d, *J* 7.7), 7.43 (2H, d, *J* 7.2), 7.34 (2H, dd, *J* 7.5, 7.5), 7.30–7.20 (3H, m), 3.61 (4H, br s), 2.19 (3H, s); δ_C(125 MHz, $CDCl_3$) 157.8 (s), 149.6 (s), 148.1 (s), 138.8 (s), 137.8 (s), 130.3 (d), 129.0 (d), 128.3 (d), 127.1 (d), 119.5 (d), 61.9 (t), 61.2 (t), 42.2 (q); *m*/*z* (MALDI-TOF) 362 (MH^+, 49%), 360 (M^+−1, 100), 267 (4), 243 (28), 241 (65), 91 (3).

For the preparation of (6*H*-1,2,3-benzodithiazol-6-ylidene)propanedinitriles, **54** and **55**, substituted 6-chloro-1,2,3-benzodithiazol-2-ium chlorides **II** (Herz salts) were condensed with malononitrile (1 equiv) in the presence of base (2 equiv) according to the following general procedure: To a stirred suspension of the appropriate 6-chloro-1,2,3-benzodithiazol-2-ium chloride **II** (1 mmol) in dichloromethane (25 mL) at *ca.* 20 °C, malononitrile (66 mg, 1 mmol) was added followed by the addition of Hünig's base (348 μL, 2 mmol). After 1 h the reaction mixture adsorbed onto silica and dry flash chromatography gave the corresponding (6*H*-1,2,3-benzodithiazol-6-ylidene)propane-dinitriles **54** or **55**. Analytical and spectroscopic data of the (6*H*-1,2,3-benzodithiazol-6-ylidene)propanedinitriles **54** and **55** have been previously reported [19] (Fig. 1B).

*2.2.3. Synthesis of 1,2,4-dithiazines **56**–**59***

The synthesis of 1,2,4-dithiazines **56–59** has been recently reported, [20] and involves the reaction of the appropriate (*Z*)-*N*-(4-chloro-5*H*-1,2,3-dithiazol-5-ylidene)-1*H*-pyrazol-5-amine **III** with diethylamine followed by treatment with concd H_2SO_4 according to the following general procedure: To a stirred suspension of the appropriate (*Z*)-*N*-(4-chloro-5*H*-1,2,3-dithiazol-5-ylidene)-1*H*-pyrazol-5-amine (0.2 mmol) in MeCN (4 mL) at *ca.* 20 °C was added Hünig's base (34.5 μL, 0.2 mmol) followed by diethylamine (63.0 μL, 0.6 mmol). After complete consumption of the starting material, to the mixture was added in one portion concd H_2SO_4 (55 μL, 1 mmol). The mixture was stirred for 5 min and then adsorbed onto silica and chromatographed to give the corresponding 5*H*-pyrazolo[3,4-*e*][1,2,4]dithiazine-3-carbonitrile. Analytical and spectroscopic data of the 1,2,4-dithiazines **56–59** have been previously reported [20] (Fig. 1C).

2.3. Purification of hLAT1

hLAT1 wild type and mutants C335A, C407A and C335A/C407A over-expressed in *E. coli* were purified as previously described [9]. After cell lysate solubilisation and centrifugation (12,000*g*, 10 min, 4 °C), the purification was performed using ÄKTA start. In particular, the supernatant was applied on a His Trap HP column (5 ml Ni Sepharose) equilibrated with 10 mL buffer (20 mM Tris HCl pH 8.0, 10% glycerol, 200 mM NaCl, 0.1% sarkosyl, and DTE 2 mM) while the protein was eluted with the same buffer plus 400 mM imidazole. Desalt of 2.5 mL of the purified protein was than performed using a PD-10 column.

2.4. Reconstitution of the purified hLAT1

The purified hLAT1 was reconstituted by removing detergent from mixed micelles containing detergent, protein and phospholipids using batch/wash method as previously described [9]. The initial mixture contained: 4 μg of purified protein, 100 μL of 10% $C_{12}E_8$, 100 μL of 10% egg yolk phospholipids (*w*/*v*) in the form of liposomes prepared as previously described [21], 20 mM Tris HCl pH 7.5 and 10 mM L-His in a final volume of 700 μL. This mixture composition led to a final intraliposomal His concentration of 10 mM that was the optimal condition for accumulation of the externally added radioactive His (see below) by the antiport transport mechanism [11].

2.5. Transport measurements

To remove the external substrate, 600 µL of proteoliposomes was passed through a Sephadex G-75 column (0.7 cm diameter × 15 cm height) pre-equilibrated with 20 mM Tris HCl pH 7.5 and sucrose at an appropriate concentration to balance internal osmolarity. Transport was initiated by adding 5 µM [^{3}H]His to proteoliposomes and stopped by a mixture of 100 µM BCH and 1.5 µM $HgCl_2$. In controls, the mixture of inhibitors was added at time zero according to the inhibitor stop method [22]. 100 µL of proteoliposomes was passed through a Sephadex G-75 column (0.6 cm diameter × 8 cm height) at the end of the transport assay, to separate the external from the internal radioactivity. Proteoliposomes were eluted with 1 mL 50 mM NaCl in 4 mL scintillation mixture and counted. For [^{3}H]His uptake analysis, experimental values were corrected by subtracting controls. Initial transport rate was measured by stopping the reaction after 15 min for wild type protein and after 30 min for Cys mutants, *i.e.*, within the initial linear range of [^{3}H]His uptake in proteoliposomes. Grafit 5.0.13 software was used to calculate kinetic parameters and derive IC_{50} values in inhibition assays. Protein concentration was estimated by Chemidoc imaging system to calculate the hLAT1 specific activity [23].

2.6. Cell culture

HEK293 and SiHa cells, at late passage and kindly provided by Dr. Massimo Tommasino Infection and Cancer Biology group (IARC/CIRC-WHO/OMS), were maintained in Dulbecco's Modified Eagle Medium (DMEM) supplemented with 10% (*v*/*v*) fetal bovine serum (FBS), 1 mM glutamine and 1 mM sodium pyruvate and Pen/Strep as antibiotics. Cells were grown on 10 cm^2 plates at 37 °C in a humidified incubator and a 5% CO_2 atmosphere.

2.7. Transport measurement in HEK293 cells

pCDNA3hLAT1-HA was obtained by subcloning the cDNA of hLAT1 between BamHIII and XhoI restriction site into pCDNA3 mammalian expression vector. The HA tag was added by two sequential PCR reaction using the reverse 1 ATCTGGAACATCGTATGGGTATGTCTCCTGGGGGACCAC, then the reverse 2 CGGTCTCGAGCTAAGCGTAATCTGGAACATCGTATGGGTA and a single forward CGCGGATCCACCATGGCGGGTGCGGGCCCGAAG. The construct was verified by DNA sequencing. HEK293 cells were seeded onto 10 cm^2 plates and cultured using standard culturing conditions until they reached 80% confluence. Cells were transfected with Polyjet (Signagen Laboratories) transfection reagent according to the manufacturer's procedures with 5 µg of pCDNA3hLAT1-HA or empty vector. After 24 h, empty vector or hLAT1 expressing cells were seeded onto 12 well plates and used for transport assay of L-[^{3}H]His. Cells were rinsed twice with warm transport buffer: 20 mM Tris HCl pH 7.4 and 5 mM glucose. Radiolabeled 5 µM [^{3}H]His was added and the transport reaction was terminated after 1 min by discarding the uptake buffer and rinsing the cells three times with the same ice-cold transport buffer (0.5 mL per well per rinse) plus 10 mM BCH. Cells from each well were solubilized in 500 µL of 1% TX-100 solution. Cell extracts were counted for radioactivity (400 µL). The remaining 100 µL in each well were used for protein concentration assay. Specific His-transport was evaluated by subtracting the transport values of cells transfected with hLAT1 to those transfected with empty vector. To verify hLAT1 over-expression, western blot analysis was conducted on cell lysates harboring or not hLAT1-HA. The protein was immuno-detected incubating membrane with anti-HA (Sigma Aldrich) antibody 1:1000 overnight at 4 °C. As loading control 1:5000 anti-Actin (Sigma Aldrich) was used 1 h at room temperature. The reactions were detected by Electro Chemi Luminescence (ECL) assay after 1 h incubation at room temperature with secondary antibody anti-mouse (Cell Signaling) 1:5000.

2.8. Cell viability

SiHa cells were seeded onto 6 well plates and cultured using standard culturing conditions until they reached 70% confluence. Cells were treated with 10 and 100 µM of dithiazole inhibitors as indicated in the figure legends. Cell viability was followed for 24 and 48 h and pictures were taken.

2.9. Computational studies

Outward-open hLAT1 structure was obtained by comparative modeling, using the AdiC crystallographic structure (RCSB PDB code: 3OB6) as a template [24].

Tested compounds were drawn and energy minimized by the Molecular Operating Environment (MOE) Builder, with the Amber10:EHT force field. Since 1,2,3-dithiazoles can react with nucleophile compounds, such as C335 and C407, the MOE Dock program was used with the covalent feature.

The top-scoring poses from the docking procedure were refined by using the MOE QuickPrep procedure aimed at refining the complex before calculating the approximate binding free energy via the GBVI/WSA dG empirical scoring function [25].

2.10. Statistical analysis

Data points of each experiments derived from samples in triplicates. Threshold for statistical significance (P value) was fixed at 0.01 according to Student's two tailed unpaired T-test. Data reported in Table 1 have been obtained from two experiments for a preliminary screening of the compounds.

3. Results

*3.1. Inhibition of the hLAT1 transporter by 1,2,3-dithiazoles **1**–**55** and 1,2,4-dithiazines **56**–**59***

Compounds **1**–**59** (Table 1) were prepared and tested as inhibitors of hLAT1. Transport activity was measured in proteoliposomes as [^{3}H]His_{ex}/His_{in} antiport. This assay is more suitable than using Leu or Phe for transport detection, as recently described [11]. Results from a preliminary screening of compounds at 100 µM concentrations are reported in Table 1, as percent of inhibition. The concentration used was about three times the threshold considered as significant for xenobiotic/protein interactions [26]. Several compounds triggered virtually complete inhibition, *i.e.* >90% (Table 1, compounds **5**, **10**, **11**, **12**, **16**, **17**, **19** and **59**); the other molecules led to variable inhibition, ranging from 0 to 89%. No effect was observed in the presence of DMSO, used to solubilize the compounds, demonstrating that the inhibition was exclusively caused by the compounds.

3.2. Dose-response analysis

Compounds causing inhibition higher than 90% at 100 µM were selected for dose-response analysis.

In these experiments, the rate of the [^{3}H]His/His antiport was measured in the presence of increasing concentrations of the in-

Table 1
Inhibition of hLAT1 by 1,2,3-dithiazoles **1**–**55** and 1,2,4-dithiazines **56**–**59**.

Entry	Structure	%Inhibition at 100 μM
1	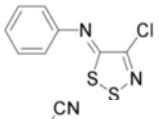	81–82
2	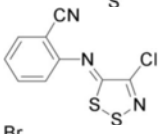	44–45
3	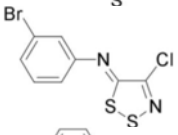	82–83
4	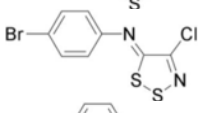	68–69
5	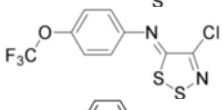	>90
6	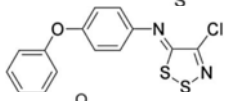	62–63
7	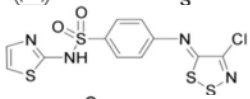	63–64
8	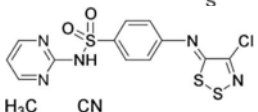	81–82
9	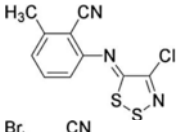	63–64
10	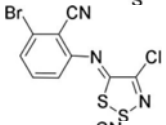	>90
11	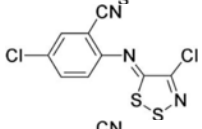	>90
12	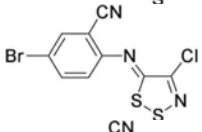	>90
13	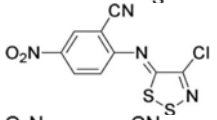	88–89
14	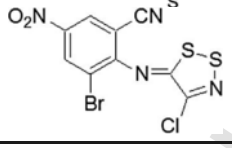	85–86

Table 1 (*Continued*)

Entry	Structure	%Inhibition at 100 μM
15	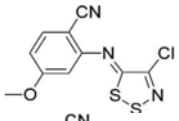	85–86
16	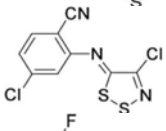	>90
17	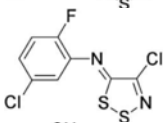	>90
18	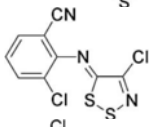	78–79
19	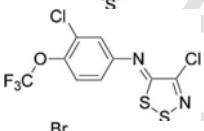	>90
20	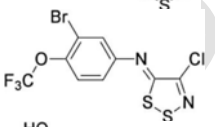	68–71
21	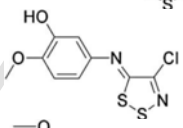	31–33
22	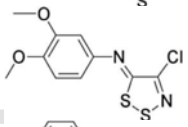	67–69
23	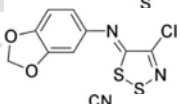	49–51
24	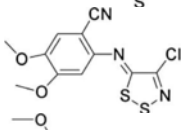	83–84
25	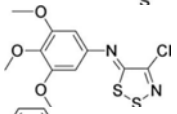	65–66
26	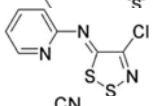	4–9
27	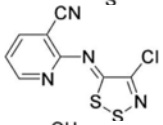	41–49
28	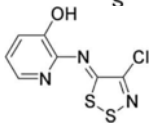	35–45

Table 1 (*Continued*)

Entry	Structure	%Inhibition at 100 μM
29	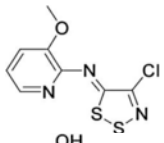	10–15
30	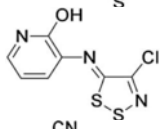	67–68
31	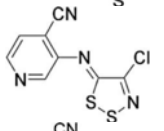	87–89
32	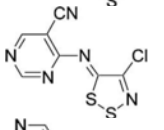	75–79
33	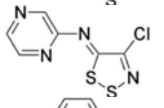	63–66
34	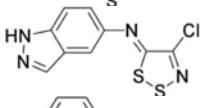	29–31
35	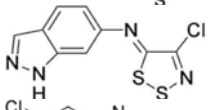	48–49
36	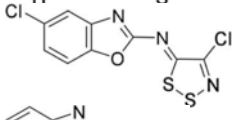	66–67
37	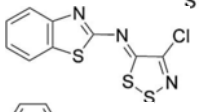	67–68
38	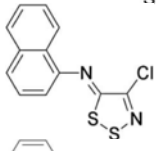	59–61
39	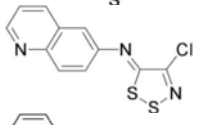	58–59
40	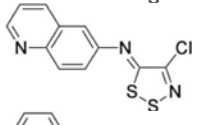	74–75
41	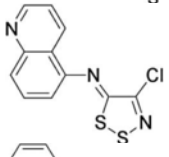	65–66
42	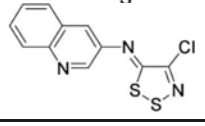	84–85

Table 1 (*Continued*)

Entry	Structure	%Inhibition at 100 μM
43	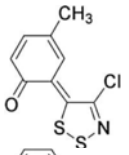	70–71
44	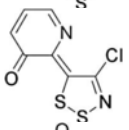	48–49
45	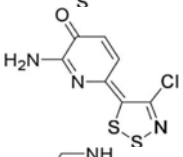	63–66
46	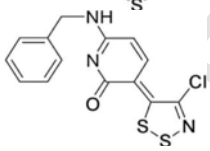	66–69
47	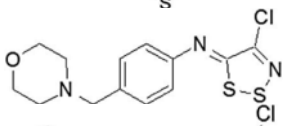	61–62
48	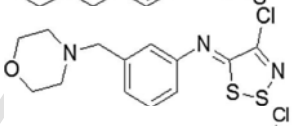	58–59
49	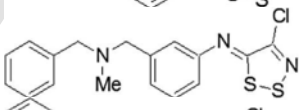	51–52
50	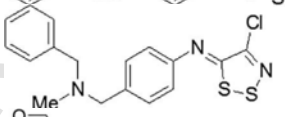	48–49
51	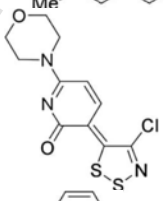	26–30
52	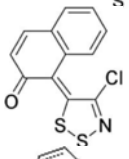	72–73
53	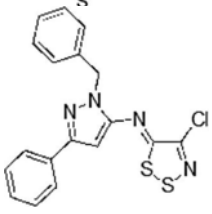	48–49

Table 1 (*Continued*)

Entry	Structure	%Inhibition at 100 μM
54	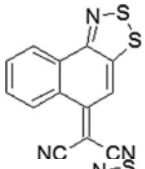	60–62
55	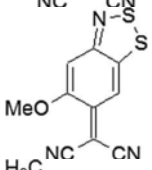	0
56	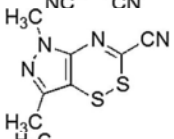	88–89
57	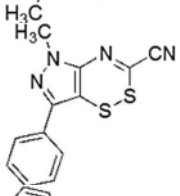	71–72
58	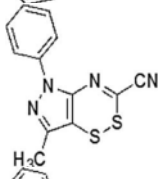	77–78
59	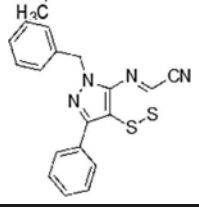	>90

Compounds structures (1–59) prepared as described in Section 2 were tested as inhibitors of hLAT1 at 100 μM concentration. Transport activity was assayed in proteoliposomes as [3H]His_{ex}/His_{in} antiport as described in Section 2. Percentage of inhibition from two experiments is reported (see Section 2.10). >90% is reported in case of both values higher than 90%.

hibitors (Fig. 2). As expected, all the selected compounds led to a strong and complete inhibition with IC_{50} values of: 0.98 ± 0.10, 1.33 ± 0.33, 1.62 ± 0.43, 2.10 ± 0.58, 1.62 ± 0.30, 0.89 ± 0.33, 1.87 ± 0.09 and 5.2 ± 0.11 μM for compounds **5**, **10**, **11**, **12**, **16**, **17**, **19** and **59**, respectively (Fig. 2).

3.3. Molecular mechanism of interaction/inhibition

Dithiazoles and dithiazines are expected to interact with the protein through formation of mixed disulfide/trisulfide as previously reported ([14,27,28] and see Fig. 3). Human LAT1 harbors 12 Cys residues in its structure; thus, a strategy for assessing the possible reaction with thiol residues was adopted (Fig. 4): after size exclusion chromatography, proteoliposomes were incubated with or without the two most potent inhibitors, *i.e.* compounds **5** and **17** of Table 1. Then, the samples were incubated further with or without the disulfide reducing agent DTE. After incubations, excess of unreacted compounds was removed by a second size-exclusion chromatography. Then, His transport was assayed as described above. Permanence of inhibition after this procedure indicated formation of covalent bond(s) between the inhibitor and the transporter. Removal of inhibition by DTE indicated that the covalent bond was a disulfide (Fig. 5). The concentration of compounds was chosen little higher than the IC_{50} to carry out experiments under conditions of strong inhibition. As shown in Fig. 4, compounds **5** (Fig. 5A) and **17** (Fig. 5B) led to inhibition of about 75% which remained stable, *i.e.*, inhibition was still present after removal of the compounds by the second size exclusion chromatography (Fig. 4). Recovery of transport activity after addition of DTE (Fig. 5), confirmed that inhibition was caused by formation of mixed di(tri)sulfides (see Fig. 3).

3.4. Kinetics of inhibition

To gain further insights into the molecular mechanisms, inhibition kinetics was investigated. The dependence of transport rate on His concentration in the presence of the compounds **5** and **17** at concentrations close to their IC_{50} (Fig. 6) was studied. The data are reported in double reciprocal plots, according to Lineweaver-Burk. Straight line patterns intersecting on, or close to, the *x*-axis were found, indicating mixed or non-competitive inhibition for compound **5** (Fig. 6A) and mixed inhibition for compound **17** (Fig. 6B). The half saturation constants K_i, calculated from the experiments were 0.76 ± 0.27 μM and 1.13 ± 0.41 μM for compounds **5** and **17**, respectively (Fig. 6A-B). The possible protection of inhibition by substrate was tested: pre-incubation of proteoliposomes with His at concentrations up to 10 mM was performed prior to dithiazoles addition. No protection was observed on inhibition by compound **5** (Fig. 6C), in agreement with the covalent mechanism of action and the non-competitive pattern.

3.5. Homology model and effects on LAT1 mutants

The reactivity of dithiazoles towards SH groups of the protein allowed hypothesizing the involvement of one or more Cys residues as the nucleophilic groups responsible for attacking the cyclic disulfide bond of the inhibitor. The availability of 3D homology model [9] allowed us to perform covalent docking simulations both on C335 and C407 for compounds **5** and **17**. The analysis showed that both compounds **5** and **17** can bind to C407 (covalent docking score and approximate binding free energy for compound **5**: −4.8 kcal/mol and −21.4 kcal/mol, respectively; covalent docking score and approximate binding free energy for compound **17**: −3.1 kcal/mol and −14.6 kcal/mol, respectively) (Fig. 7); Compound **51** was used as negative control of docking (covalent docking score, 125.6 kcal/mol) being a poor inhibitor of LAT1 (Table 1).

Interestingly, the identified residue was C407 located in the substrate binding site as previously demonstrated [9]. Thus, the C407A mutant was employed for dose-response analyses performed using compound **5**. This was chosen due to its higher affinity (K_i value), confirmed by the good covalent docking score and approximate binding free energy obtained *in silico*. The calculated IC_{50} of the C407 mutant was 3.76 ± 0.28 μM, *i.e.* four times higher than that of wild type (Fig. 8A). The substrate binding site includes also C335; however, docking analysis predicted no interaction of this residue with both compounds **5** and **17**. Indeed, IC_{50} of C335A mutant for compound **5** was 1.32 ± 0.16 μM (Fig. 8B), *i.e.* similar to that of wild type (Fig. 2A). To further ascertain the exclusive role of C407, the IC_{50} was calculated also for the double mutant C335A/C407A (Fig. 8C). In this case, a value of 4.60 ± 0.39 μM was obtained, similar to that of the single mutant C407A.

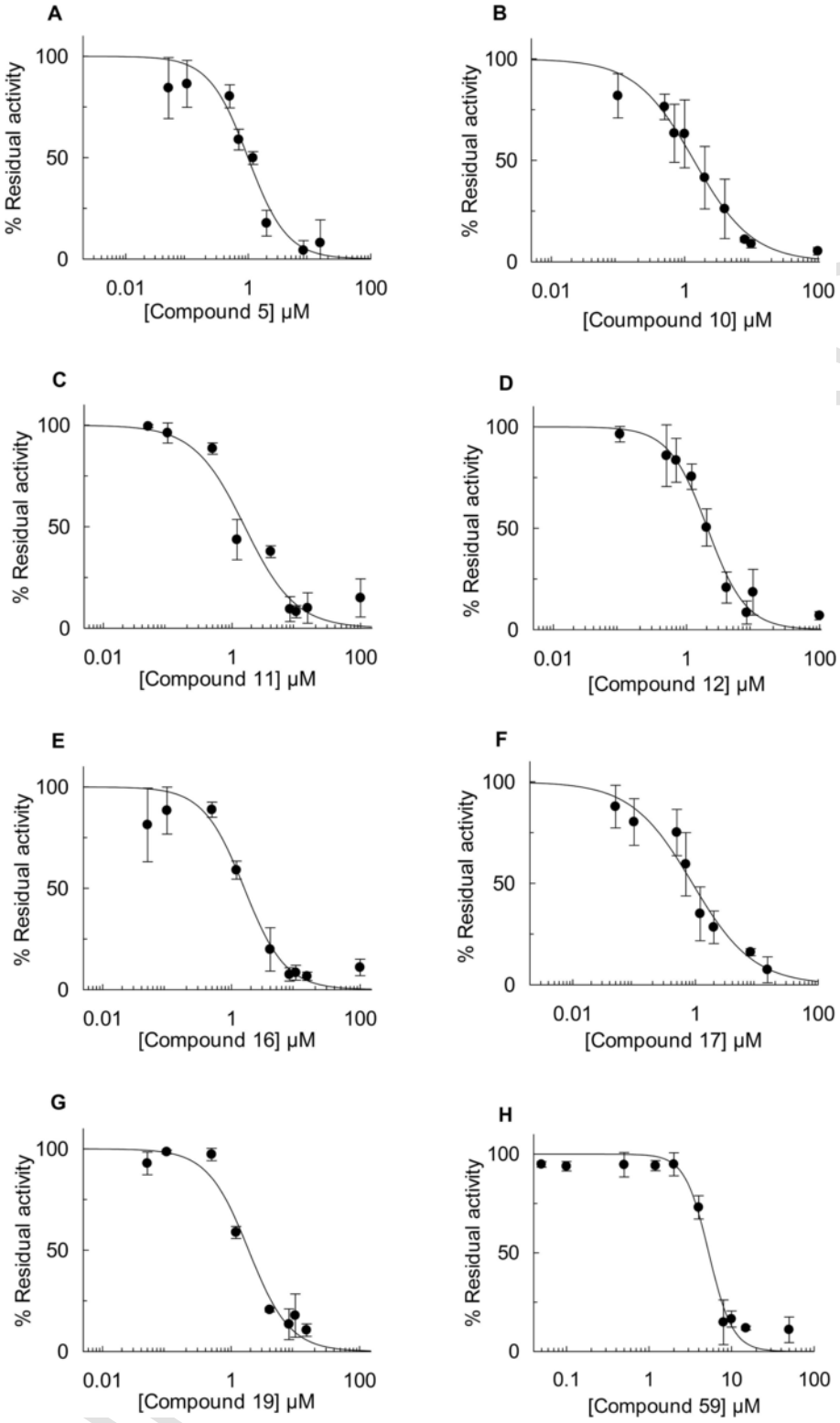

Fig. 2. Dose-response curves for the inhibition of the recombinant hLAT1 in proteoliposomes. Transport was measured adding 5 μM [^{3}H]His to proteoliposomes containing 10 mM His in the presence of different concentrations of the indicated compounds and measured in 15 min as described in Section 2. Dose-response for compound **5** (A), compound **10** (B), compound **11** (C), compound **12** (D), compound **16** (E), compound **17** (F), compound **19** (G) and compound **59** (H). Percent residual activity with respect to the control (without additions) is reported. Results are mean ± S.D. from three independent experiments.

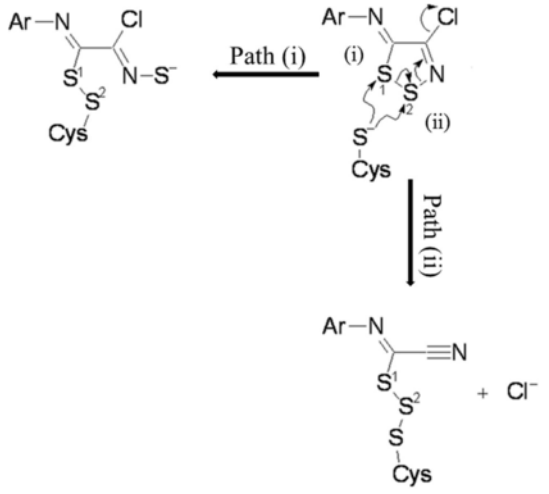

Fig. 3. Possible pathways for the mechanism of hLAT1 transporter inhibition by compounds. Cys-S, thiolate group of a Cys residue.

3.6. Effects on intact cells

Inhibition by compound **5** was tested on intact HEK293 cells transiently transfected with hLAT1-HA. Fig. 9A demonstrates the actual over expression of hLAT1 detected by an anti-HA antibody. [^{3}H]His uptake was measured in the presence or absence of compound **5** (Fig. 9B) at a concentration corresponding to its IC_{50} in proteoliposomes (Fig. 2A). Transport in HEK293 cells was inhibited by about 50% indicating that the compound inhibits hLAT1 in intact cells at the same extent of proteoliposomes. This correlates well with previous findings describing an overlapping behavior of the transporter in proteoliposomes and in intact cells [11]. To gain further insights on the biological effects of inhibitors, cell viability was tested. SiHa cell line was used because it harbors a detectable level of endogenous LAT1 [11]. The experiment was conducted by monitoring cell morphology 24 and 48 h after addition of increasing concentrations of the most active compounds **5** and **17** or the negative control compound **51** that showed <30% inhibition in proteoliposomes (Table 1); DMSO was added to control cells, *i.e.*, in the absence of inhibitor (Fig. 10). Interestingly, the compounds with the lowest IC_{50} were very effective in inducing apparent cell death triggering significant reduction of cell numbers together with evident changes in cell morphology. The effects were more pronounced after 48 h. Interestingly, after washing out the compounds, cell viability was still impaired. Compound **51** was used as specificity control being one of the compounds with the lowest inhibitory effects on LAT1. Notably, the compound did not cause cell death highlighting the specificity of the tested dithiazoles with respect to hLAT1 activity.

4. Discussion

In the last 10 years, more than 200 papers appeared on Pubmed database [“LAT1” (or aliases) and “cancer” (or aliases) as query in Title/Abstract] dealing with LAT1 over-expression in several human cancers. On this basis, the transporter was acknowledged as a new pharmacological target for cancer therapy. LAT1 has been also ex-

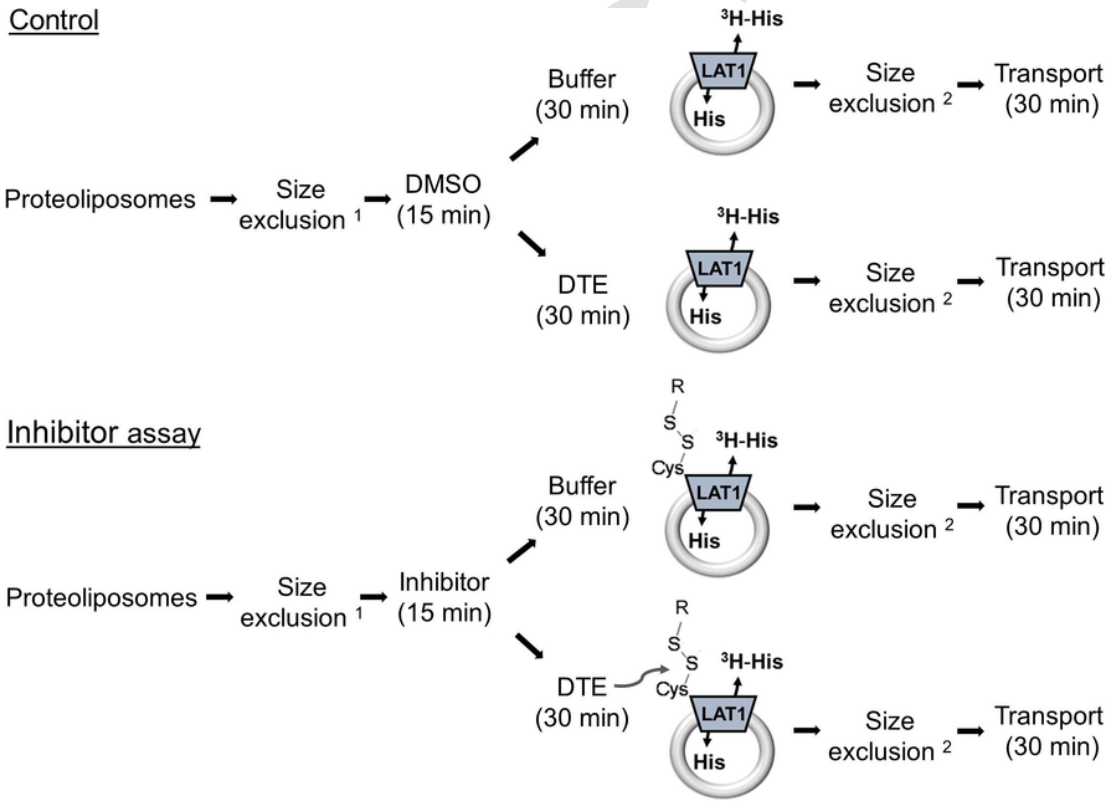

Fig. 4. Sketch of experimental design for assessing the possible reaction of the compound with thiol residues of the protein. After reconstitution, proteoliposomes were incubated with DMSO (control) or with a specific compound (Inhibition assay) for the indicated time. Later, these samples were incubated with buffer alone or with 50 mM DTE. Transport was then measured in 30 min by adding 5 μM [^{3}H]His to proteoliposomes, as described in Section 2. [1]: A first size exclusion chromatography was performed to remove the external substrate after reconstitution. [2]: A second size exclusion chromatography was performed to remove inhibitor not bound to the transporter.

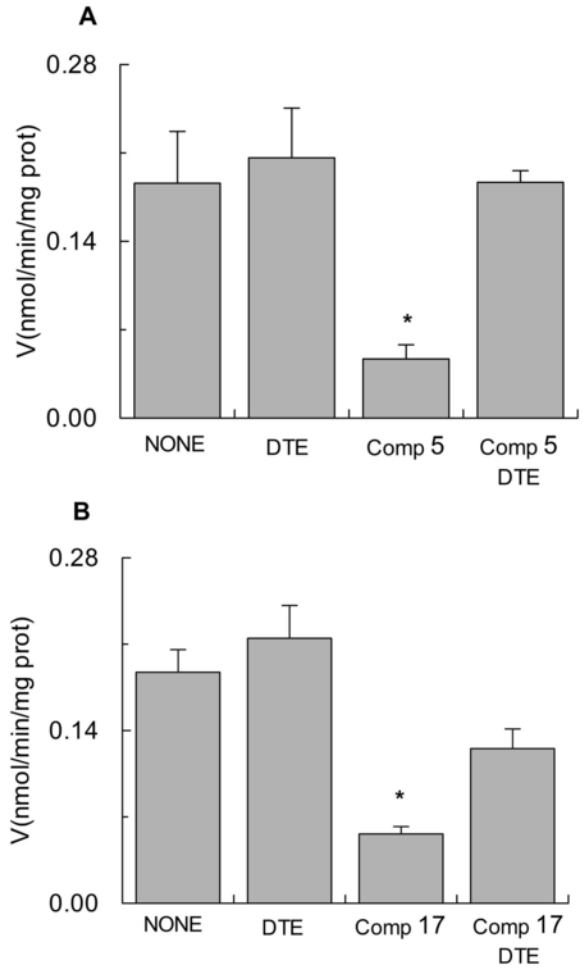

Fig. 5. Effect of DTE on the inhibition of [^{3}H]His uptake in proteoliposomes reconstituted with recombinant hLAT1. Experimental procedure is described in the legend of Fig. 3. Proteoliposomes were incubated with DMSO or with 1.2 μM compound **5** (A), 1.2 μM compound **17** (B), and not treated or treated with 50 mM DTE. Results are mean ± S.D. from three independent experiments. Student's two tailed unpaired *t*-test was performed on the sample without added compounds (control); p value was symbolized as follows: $^*p < 0.01$.

ploited for delivery of pharmacological compounds which mimic its substrates using the pro-drug approach [29]. Proteoliposomes reconstituted with hLAT1 have been adopted in the present work as the main experimental model for the screening of inhibitors. Proteoliposomes have the advantage of detecting effects exclusively ascribed to the transport protein underneath. On the other hand, some weakness of this system may be due to the absence of cell components interacting and influencing the activity of the transporter. However, in the case of hLAT1, it was previously demonstrated that it is the sole polypeptide competent for transport function of the heterodimer LAT1/CD98 [11]. Data on inhibitors have been confirmed by experimental models closer to the *in vivo* conditions.

The task of designing good ligands/inhibitors for LAT1 is challenging, as for most membrane transporters, owing to the absence of a 3D crystallographic structure. Indeed, LAT1 structures were predicted, so far, by homology modeling on the basis of the *E. coli* arginine/agmatine transporter AdiC [9,24,30–32], which shares a relatively low sequence identity with hLAT1. From these models, some features of the substrate binding site of hLAT1 were predicted. These characteristics were exploited for designing substrate-mimicking molecules, with the aim of finding potent competitive inhibitors

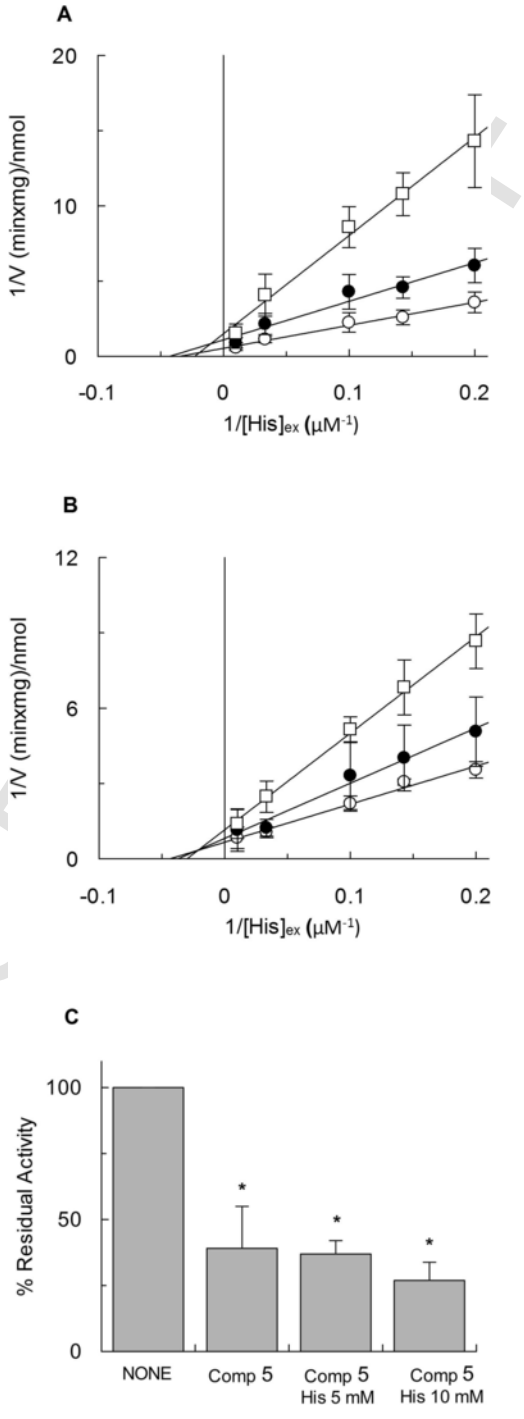

Fig. 6. Kinetic analysis of the inhibition of recombinant hLAT1 reconstituted in proteoliposomes. Data were plotted according to Lineweaver–Burk as reciprocal transport rate vs reciprocal His concentration. Transport rate was measured by adding [^{3}H]His at the indicated concentrations to proteoliposomes containing 10 mM His and stopping the reaction after 15 min as described in Section 2. In (A) 0.8 μM (●) or 1.2 μM (□) **5** was added in comparison to samples without inhibitor (○). In (B) 0.8 μM (●) or 1.2 μM (□) **17** was added in comparison to samples without inhibitor (○). Results are mean ± S.D. from three independent experiments. (C) Protection of inhibition by substrate. Proteoliposomes reconstituted as described in Section 2, were incubated or not with compound **5** in the presence or absence of **5** or 10 mM His. After incubation, samples were subjected to size exclusion chromatography to remove the unreacted inhibitor and substrate; transport rate was measured adding 5 μM [^{3}H]His. The reaction was stopped after 30 min as described in Section 2. Percent residual activity with re-

spect to the control (without additions) is reported. Results are mean ± S.D. from three independent experiments. Student's two tailed unpaired *t*-test was performed on the sample without added compounds (control); p value was symbolized in (C) as follows: $^{*}p < 0.01$.

[13,33–36]. A similar strategy was firstly used for designing inhibitors of the ASCT2 amino acid transporter [37]. These inhibitors present a limitation caused by the competition exerted by endogenous amino acid substrates which have plasma concentrations higher than the K_m for the transporters [4,38]. In this condition, inhibitors can be displaced from the transporter site leading to only transient or scarce effects [33]. Herein, an alternative strategy has been attempted taking into account the information recently obtained on structure-function relationships of hLAT1 substrate site [9]. Indeed, we exploited the presence of Cys residues in the substrate binding site of the protein to obtain, on the one hand, a more potent inhibition in terms of affinity, on the other hand, an irreversible inhibition mechanism to chemically knocking-out the transporter. Thus, a number of electrophilic molecules have been tested, likely reacting covalently with the thiolate group of a Cys, that are dithiazoles and dithiazines, known for their antibacterial, antifungal, herbicidal and anticancer effects [39–47]. Noteworthy, some of these compounds were previously described as covalent inhibitors of rat ASCT2 transporter [14]. The structures of dithiazoles and dithiazines are quite different from that of the prototype inhibitor of LAT1, BCH. However, these compounds have an imidazole-like ring, mimicking the His side chain, which may direct some of the inhibitors to the substrate binding site.

The variety of chemical substituents on the 1,2,3-dithiazole and to a lower extent on the 1,2,4-dithiazine rings allowed us to discover a number of compounds with a very high affinity for hLAT1 showing the lowest IC_{50} achieved so far, *i.e.*, half the previous lowest value [34]. Regarding the reactivity of the compounds, the S2 atom of the disulfide motif (Fig. 3), would represent the preferred electrophilic site for the attack by a thiolate of a Cys residue of the protein; however, the nucleophilic attack on S1 cannot be excluded. The reaction mechanism may therefore occur via the formation of mixed di- or trisulfides, as previously suggested for the reaction of the same compounds with another amino acid transporter [14]. The mixed disulfide mechanism has been adopted (Fig. 3) for docking calculations since this is the most widely occurring mechanism *in vivo*. The covalent interaction was demonstrated herein for the most effective compounds **5** and **17**. Three different strategies were adopted to identify the mechanism of inhibition and the Cys residue(s) targeted by these compounds. Firstly, the significant activity recovery induced by the thiol reducing agent DTE indicated involvement of Cys residue(s) in the covalent interaction with compounds. However, in the case of compound **17**, DTE did not allow 100% recovery of hLAT1 transport

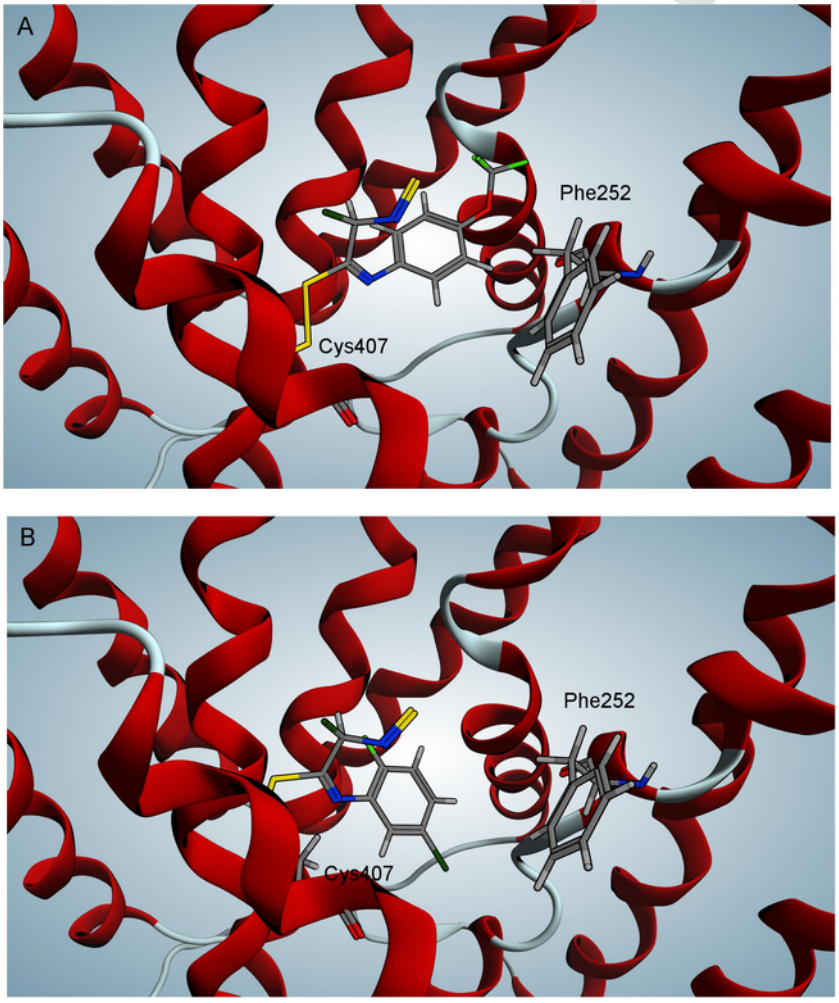

Fig. 7. Best docking poses of the two selected compounds obtained through covalent docking on LAT1 homology model. LAT1 in its outward-open conformation is shown as ribbon; the gate residue Phe252 is shown in stick representation. Compounds **5** and **17** covalently docked to residue Cys407 are shown in stick representation in A and B, respectively.

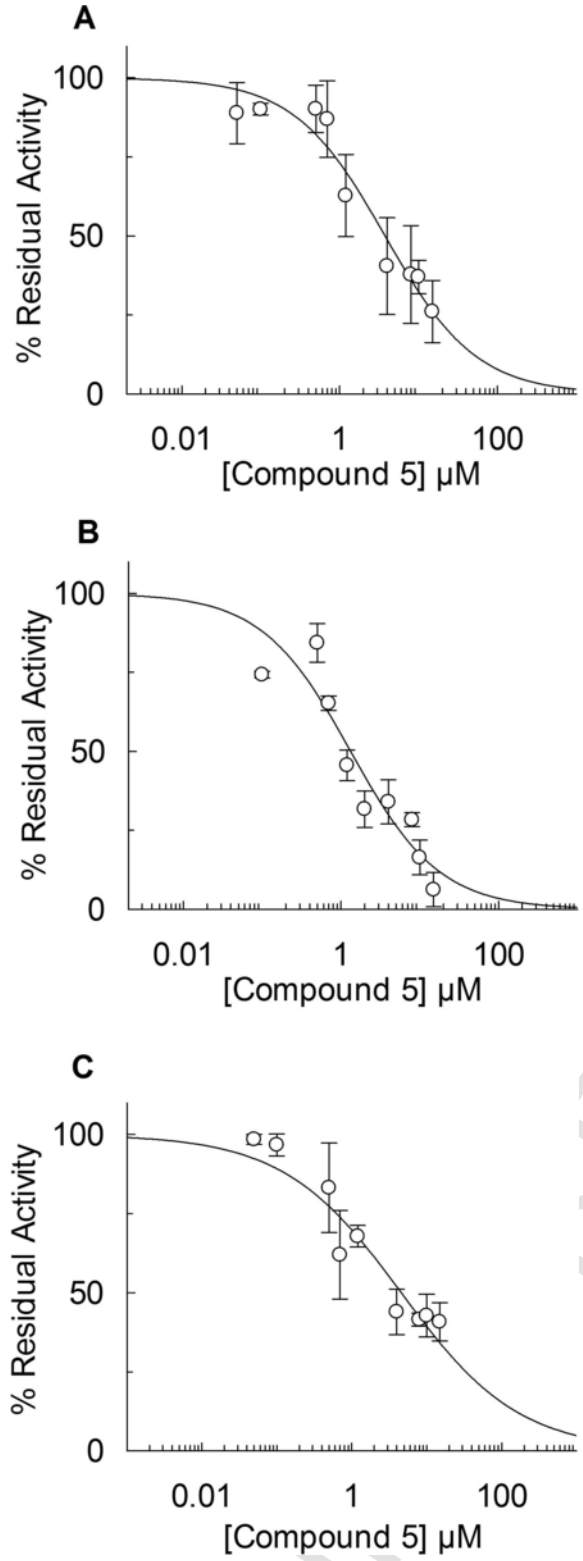

Fig. 8. Inhibition analysis of compound **5** on recombinant hLAT1 mutants reconstituted in proteoliposomes. Dose-response curve for the inhibition of compound **5** on LAT1 C407A (A), on C335A (B) and on double mutant C335A/C407A (C). Transport was measured by adding 5 μM [^{3}H]His to proteoliposomes containing 10 mM His in the presence of different concentrations of the compounds added together with [^{3}H]His and measured in 30 min as described in Section 2. Percent residual activity with respect to the control (without additions) is reported. Results are mean ± S.D. from three independent experiments.

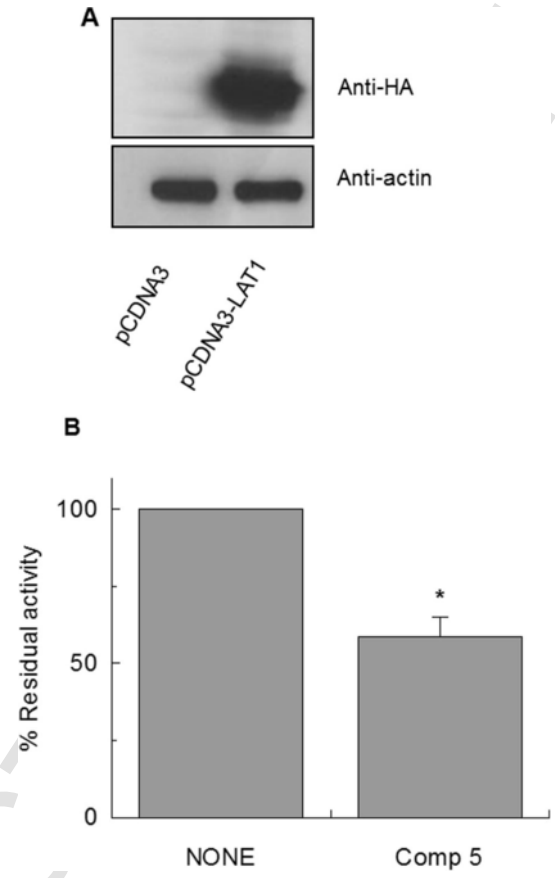

Fig. 9. Effect of compound **5** on transport activity in intact cells. (A) Western Blot analysis was conducted using anti-HA antibody on cells transfected with empty vector (pCDNA3) or hLAT1-HA (pCDNA3-LAT1) as described in Section 2. Actin is used as loading control. Picture is representative of three independent experiments. (B) HEK293 cells were cultured and transfected with pCDNA3-hLAT1-HA as described in Section 2 and used for transport adding 5 μM[^{3}His] and 1 μM of compound 5. Transport was stopped after 1 min as described in Section 2. Results are mean ± S.D. from three independent experiments. Student's two tailed unpaired *t*-test was performed on the sample without added compound (control); p value was symbolized as follows: $^*p < 0.01$.

activity probably because of additional hydrophobic interactions independent from thiol reactivity. Secondly, the kinetics showed a non-competitive and mixed type inhibition for both compounds **5** and **17** that supported the covalent interaction with hLAT1. In line with this experimental data, C407 was identified as the target of compound **5** by site-directed mutagenesis.

C407 is located in the substrate binding site, therefore it may be easily blocked by mixed sulfide formation triggering the competitive component of the inhibition. Accordingly, the pre-incubation of reconstituted proteoliposomes with excess of substrate did not alter the inhibition potency by compounds **5**. Even though many proteins have exposed Cys thiol groups, the specificity of these compounds towards hLAT1 may be conferred by the peculiar localization of C407 in the substrate binding site.

Some information on SAR trends can be obtained from the IC_{50} of the eight most active compounds and from the % of inhibition by all the others. It seems likely that electron withdrawal substituents on the phenyl ring facilitate the interaction/binding to the protein resulting in a higher inhibitory effect, with the exception of compound **2**. In

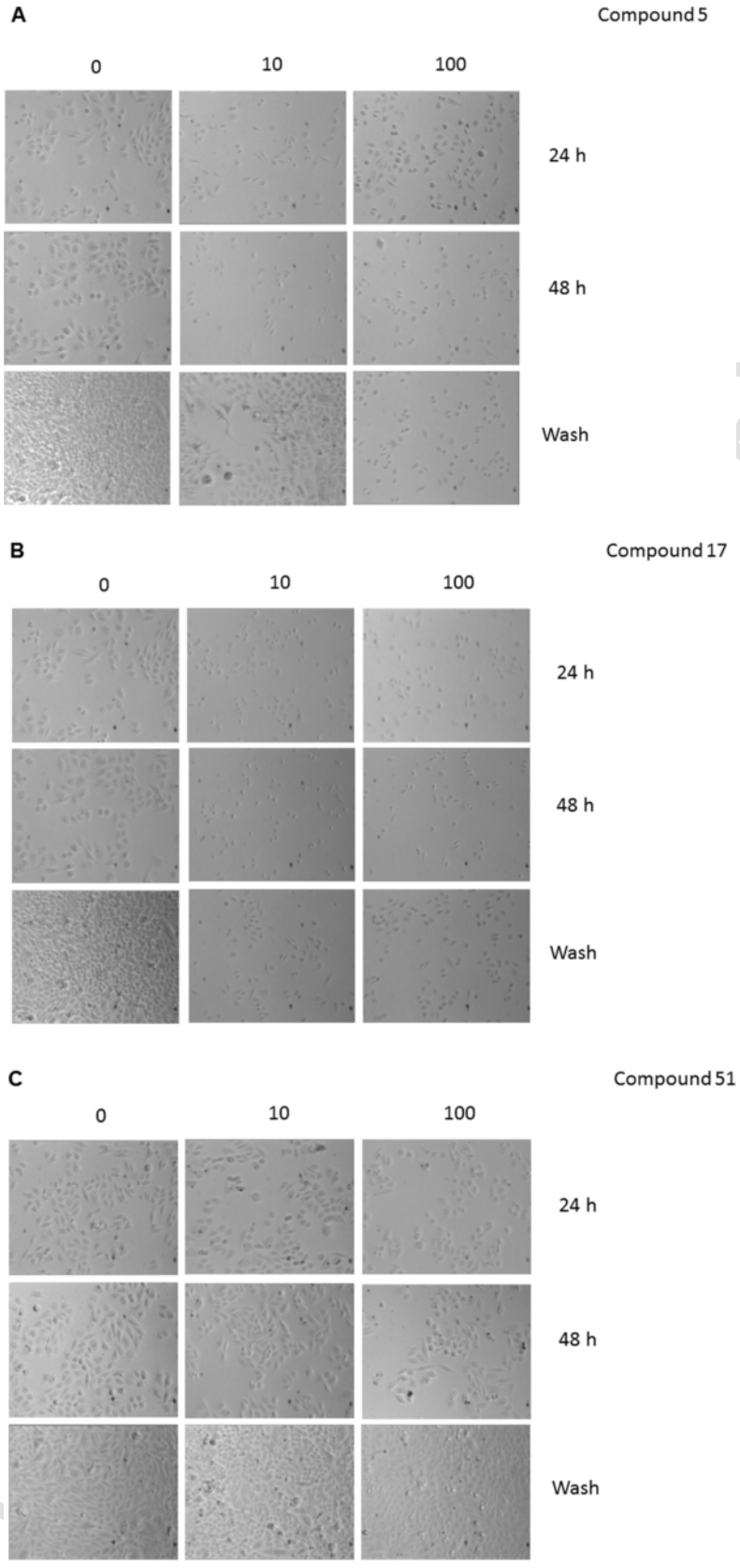
A
Compound 5
0
10
100
24 h
48 h
Wash
B
Compound 17
0
10
100
24 h
48 h
Wash
C
Compound 51
0
10
100
24 h
48 h
Wash

Fig. 10. Effect of compounds on cell viability. SiHa cells were cultured in 6 well plates as described in Section 2. Compounds **5** (A), **17** (B) and **51** (C) were added at the indicated concentrations and pictures were taken after 24 h and 48 h of treatment. As negative control, DMSO was added. After 48 h medium was replaced with fresh DMEM without inhibitors (wash) and pictures were taken after 24 h. Picture is representative of three independent experiments.

contrast, electron-donating and bulky substituents, along with polycyclic compounds, are in general less effective in blocking LAT1 transport activity. The pyrid-2-yl sp^2 nitrogen lone pair of dithiazoles **26**–**29**, **32** and **33** donates electron density into the antibonding S—S bond of the dithiazole and this raises the electron density of the ring, making it less prone to thiophilic attack. This explains the sudden drop in activity of such dithiazoles while, interestingly, the introduction of electron withdrawing groups (such as the cyano group in **27**) restores some activity. This electronic effect was recently detected in the evaluation of 1,2,3-dithiazoles reactivity [28].

Interestingly, the strategy adopted in this work responded also to the 3R requirement for animal testing: Replace, Reduce, Refine. In fact, out of 59 compounds 8 hits were identified and, among them, 2 lead compounds were selected for a deep investigation. Only at the very end of the screening, the selected compounds, for which the molecular mechanism of action was deciphered in proteoliposomes, were tested on cell viability. Data on cells correlate well with the specific potency of the most effective compounds characterized in the *in vitro* system. The described study identifies, with relatively low cost and no animal experimentation, the molecular scaffold that could be used for designing potential drugs for more advanced pre-clinical trials.

Conflicts of interest

The authors declared that they have no competing interests.

Acknowledgements

This work was supported by Ministry of Instruction University and Research (MIUR)-Italy, by a grant from PON-ricerca e competitività 2007–2013 (PON project 01_00937: "Modelli sperimentali biotecnologici integrati per la produzione ed il monitoraggio di molecole di interesse per la salute dell'uomo"). PK and MK thank the Cyprus Research Promotion Foundation (Grant: NEKYP/0308/02) and the following organizations and companies in Cyprus for generous donations of chemicals and glassware: the State General Laboratory, the Agricultural Research Institute, the Ministry of Agriculture, MedoChemie Ltd, Medisell Ltd and Biotronics Ltd. Furthermore, we thank the A. G. Leventis Foundation for helping to establish the NMR facility at the University of Cyprus.

References

[1] D. Fotiadis, Y. Kanai, M. Palacin, The SLC3 and SLC7 families of amino acid transporters, Mol. Asp. Med. 34 (2–3) (2013) 139–158.
[2] R. Milkereit, A. Persaud, L. Vanoaica, A. Guetg, F. Verrey, D. Rotin, LAPTM4b recruits the LAT1-4F2hc Leu transporter to lysosomes and promotes mTORC1 activation, Nat. Commun. 6 (2015) 7250.
[3] Y.D. Bhutia, E. Babu, S. Ramachandran, V. Ganapathy, Amino Acid transporters in cancer and their relevance to "glutamine addiction": novel targets for the design of a new class of anticancer drugs, Cancer Res. 75 (9) (2015) 1782–1788.
[4] M. Scalise, L. Pochini, M. Galluccio, C. Indiveri, Glutamine transport. From energy supply to sensing and beyond, Biochim. Biophys. Acta 1857 (8) (2016) 1147–1157.
[5] B.C. Fuchs, B.P. Bode, Amino acid transporters ASCT2 and LAT1 in cancer: partners in crime?, Semin. Cancer Biol. 15 (4) (2005) 254–266.
[6] Y. Zhao, L. Wang, J. Pan, The role of L-type amino acid transporter 1 in human tumors, Intractable Rare Dis. Res. 4 (4) (2015) 165–169.
[7] V. Ganapathy, M. Thangaraju, P.D. Prasad, Nutrient transporters in cancer: relevance to Warburg hypothesis and beyond, Pharmacol. Ther. 121 (1) (2009) 29–40.
[8] L. Yang, T. Moss, L.S. Mangala, J. Marini, H. Zhao, S. Wahlig, G. Armaiz-Pena, D. Jiang, A. Achreja, J. Win, R. Roopaimoole, C. Rodriguez-Aguayo, I. Mercado-Uribe, G. Lopez-Berestein, J. Liu, T. Tsukamoto, A.K. Sood, P.T. Ram, D. Nagrath, Metabolic shifts toward glutamine regulate tumor growth, invasion and bioenergetics in ovarian cancer, Mol. Syst. Biol. 10 (2014) 728.
[9] L. Napolitano, M. Galluccio, M. Scalise, C. Parravicini, L. Palazzolo, I. Eberini, C. Indiveri, Novel insights into the transport mechanism of the human amino acid transporter LAT1 (SLC7A5) Probing critical residues for substrate translocation, Biochim. Biophys. Acta 1861 (4) (2017) 727–736.
[10] D.C. Tarlungeanu, E. Deliu, C.P. Dotter, M. Kara, P.C. Janiesch, M. Scalise, M. Galluccio, M. Tesulov, E. Morelli, F.M. Sonmez, K. Bilguvar, R. Ohgaki, Y. Kanai, A. Johansen, S. Esharif, T. Ben-Omran, M. Topcu, A. Schlessinger, C. Indiveri, K.E. Duncan, A.O. Caglayan, M. Gunel, J.G. Gleeson, G. Novarino, Impaired amino acid transport at the blood brain barrier is a cause of autism spectrum disorder, Cell 167(6) (2016) 1481–1494 e18.
[11] L. Napolitano, M. Scalise, M. Galluccio, L. Pochini, L.M. Albanese, C. Indiveri, LAT1 is the transport competent unit of the LAT1/CD98 heterodimeric amino acid transporter, Int. J. Biochem. Cell Biol. 67 (2015) 25–33.
[12] J. Fort, L.R. de la Ballina, H.E. Burghardt, C. Ferrer-Costa, J. Turnay, C. Ferrer-Orta, I. Uson, A. Zorzano, J. Fernandez-Recio, M. Orozco, M.A. Lizarbe, I. Fita, M. Palacin, The structure of human 4F2hc ectodomain provides a model for homodimerization and electrostatic interaction with plasma membrane, J. Biol. Chem. 282 (43) (2007) 31444–31452.
[13] E.G. Geier, A. Schlessinger, H. Fan, J.E. Gable, J.J. Irwin, A. Sali, K.M. Giacomini, Structure-based ligand discovery for the Large-neutral Amino Acid Transporter 1, LAT-1, Proc. Nat. Acad. Sci. U.S.A. 110 (14) (2013) 5480–5485.
[14] F. Oppedisano, M. Catto, P.A. Koutentis, O. Nicolotti, L. Pochini, M. Koyioni, A. Introcaso, S.S. Michaelidou, A. Carotti, C. Indiveri, Inactivation of the glutamine/amino acid transporter ASCT2 by 1,2,3-dithiazoles: proteoliposomes as a tool to gain insights in the molecular mechanism of action and of antitumor activity, Toxicol. Appl. Pharmacol. 265 (1) (2012) 93–102.
[15] L. Pochini, M. Scalise, M. Galluccio, C. Indiveri, Membrane transporters for the special amino acid glutamine: structure/function relationships and relevance to human health, Front. Chem. 2 (2014) 61.
[16] J.H. Appel R., Siray M., Knoch F., Synthesis and reactions of 4,5-dichloro-1,2,3-dithiazolium chloride, Chem. Ber. Recl., 118 (1985) 1632–1643.
[17] O.A. Rakiti, R.F. English, C.W. Rees, O.G. Vlasova, Conversion of imino-1,2,3-dithiazoles into 2-cyanobenzothiazoles, cyanoimidoyl chlorides and diatomic sulfur, J. Chem. Soc. Perkin Trans. 1 (1997) 201–205.
[18] P.A. Koutentis, M. Koyioni, S.S. Michaelidou, Synthesis of [(4-chloro-5H-1,2,3-dithiazol-5-ylidene)amino]azines, Molecules 16 (11) (2011) 8992–9002.
[19] C.W. Rees, P.A. Koutentis, Reaction of Herz salts with malononitrile: a general route to (6H–1,2,3-benzodithiazol-6-ylidene)malononitriles, J. Chem. Soc. Perkin Trans. 1 (2002) 315–319.
[20] M. Koyioni, M. Manoli, P.A. Koutentis, Synthesis of fused 1,2,4-dithiazines and 1,2,3,5-trithiazepines, J. Org. Chem. 79 (20) (2014) 9717–9727.
[21] C. Indiveri, G. Prezioso, T. Dierks, R. Kramer, F. Palmieri, Kinetic characterization of the reconstituted dicarboxylate carrier from mitochondria: a four-binding-site sequential transport system, Biochim. Biophys. Acta 1143 (3) (1993) 310–318.
[22] F. Palmieri, C. Indiveri, F. Bisaccia, V. Iacobazzi, Mitochondrial metabolite carrier proteins: purification, reconstitution, and transport studies, Methods Enzymol. 260 (1995) 349–369.
[23] E.M. Torchetti, C. Brizio, M. Colella, M. Galluccio, T.A. Giancaspero, C. Indiveri, M. Roberti, M. Barile, Mitochondrial localization of human FAD synthetase isoform 1, Mitochondrion 10 (3) (2010) 263–273.
[24] L. Kowalczyk, M. Ratera, A. Paladino, P. Bartoccioni, E. Errasti-Murugarren, E. Valencia, G. Portella, S. Bial, A. Zorzano, I. Fita, M. Orozco, X. Carpena, J.L. Vazquez-Ibar, M. Palacin, Molecular basis of substrate-induced permeation by an amino acid antiporter, Proc. Nat. Acad. Sci. U.S.A. 108 (10) (2011) 3935–3940.

[27] A. Gupta, P. Mishra, S.K. Kashaw, V. Jatav, Synthesis, Anticonvulsant, Antimicrobial and Analgesic activity of Novel 1,2,4-Dithiazoles, Indian J. Pharm. Sci. 70 (4) (2008) 535–538.

[28] M. Koyioni, M. Manoli, P.A. Koutentis, The reaction of DABCO with 4-Chloro-5H-1,2,3-dithiazoles: synthesis and chemistry of 4-[N-(2-chloroethyl)piperazin-1-yl]-5H-1,2,3-dithiazoles, J. Org. Chem. 81 (2) (2016) 615–631.

[29] L. Peura, K. Malmioja, K. Laine, J. Leppanen, M. Gynther, A. Isotalo, J. Rautio, Large amino acid transporter 1 (LAT1) prodrugs of valproic acid: new prodrug design ideas for central nervous system delivery, Mol. Pharm. 8 (5) (2011) 1857–1866.

[30] X. Gao, L. Zhou, X. Jiao, F. Lu, C. Yan, X. Zeng, J. Wang, Y. Shi, Mechanism of substrate recognition and transport by an amino acid antiporter, Nature 463 (7282) (2010) 828–832.

[31] X. Gao, F. Lu, L. Zhou, S. Dang, L. Sun, X. Li, J. Wang, Y. Shi, Structure and mechanism of an amino acid antiporter, Science 324 (5934) (2009) 1565–1568.

[32] Y. Fang, H. Jayaram, T. Shane, L. Kolmakova-Partensky, F. Wu, C. Williams, Y. Xiong, C. Miller, Structure of a prokaryotic virtual proton pump at 3.2 A resolution, Nature 460 (7258) (2009) 1040–1043.

[33] E. Augustyn, K. Finke, A.A. Zur, L. Hansen, N. Heeren, H.C. Chien, L. Lin, K.M. Giacomini, C. Colas, A. Schlessinger, A.A. Thomas, LAT-1 activity of meta-substituted phenylalanine and tyrosine analogs, Bioorg. Med. Chem. Lett. 26 (11) (2016) 2616–2621.

[34] P. Kongpracha, S. Nagamori, P. Wiriyasermkul, Y. Tanaka, K. Kaneda, S. Okuda, R. Ohgaki, Y. Kanai, Structure-activity relationship of a novel series of inhibitors for cancer type transporter L-type amino acid transporter 1 (LAT1), J. Pharm. Sci. 133 (2) (2017) 96–102.

[35] H. Ylikangas, K. Malmioja, L. Peura, M. Gynther, E.O. Nwachukwu, J. Leppanen, K. Laine, J. Rautio, M. Lahtela-Kakkonen, K.M. Huttunen, A. Poso, Quantitative insight into the design of compounds recognized by the L-type amino acid transporter 1 (LAT1), ChemMedChem 9 (12) (2014) 2699–2707.

[36] A.A. Zur, H.C. Chien, E. Augustyn, A. Flint, N. Heeren, K. Finke, C. Hernandez, L. Hansen, S. Miller, L. Lin, K.M. Giacomini, C. Colas, A. Schlessinger, A.A. Thomas, LAT1 activity of carboxylic acid bioisosteres: evaluation of hydroxamic acids as substrates, Bioorg. Med. Chem. Lett. 26 (20) (2016) 5000–5006.

[37] T. Albers, W. Marsiglia, T. Thomas, A. Gameiro, C. Grewer, Defining substrate and blocker activity of alanine-serine-cysteine transporter 2 (ASCT2) ligands with novel serine analogs, Mol. Pharmacol. 81 (3) (2012) 356–365.

[38] L.A. Cynober, Plasma amino acid levels with a note on membrane transport: characteristics, regulation, and metabolic significance, Nutrition 18 (9) (2002) 761–766.

[39] L.S. Konstantinova, O.I. Bol'shakov, N.V. Obruchnikova, H. Laborie, A. Tanga, V. Sopena, I. Lanneluc, L. Picot, S. Sable, V. Thiery, O.A. Rakitin, One-pot synthesis of 5-phenylimino, 5-thieno or 5-oxo-1,2,3-dithiazoles and evaluation of their antimicrobial and antitumor activity, Bioorg. Med. Chem. Lett. 19 (1) (2009) 136–141.

[40] J.H. Appel, R., I. Haller, M. Plempel, 1,2,3-Dithiazolderivate, Verfahren zu ihrer Herstellung Sowie ihre Verwendung als Arzneimittel, DE Pat. 2848221 (1980).

[41] C.W. Rees, T. Besson, G. Cottenceau, A.M. Pons, Antimicrobial evaluation of 3,1-benzoxazin-4-ones, 3,1-benzothiazin-4-ones, 4-alkoxyquinazolin-2-carbonitriles and N-arylimino-1,2,3-dithiazoles, Bioorg. Med. Chem. Lett. 6 (1996) 2343–2348.

[42] B. Besson, G. Cottenceau, V. Gautier, C.W. Rees, A.M. Pons, Antibacterial evaluation of novel N-arylimino-1,2,3-dithiazoles and N-arylcyanothioformamides, Bioorg. Med. Chem. Lett. 6 (1996) 529–532.

[43] K.O., Systematic Qsar procedures with quantum chemical descriptors, Quant. Struct.-Act. Relat., 6 (1987) 179–184.

[44] O.A. Rakitin, L.S. Konstantinova, Synthesis and properties of 1,2,3-dithiazoles, Russ. Chem. Rev. 77 (2008) 521–546.

[45] E. Foerster, R. Mayer, B. Matauschek, Verfahren zur Herstellung von Aromatisch oder Heteroaromatisch Substituierten Cyanthioformamiden, DD Pat. 212387 (1984).

[46] C.W. Rees, V. Thiery, T. Besson, G. Cottenceau, A.M. Pons, Antimicrobial activity of novel N-quinolinyl and N-naphthylimino-1,2,3-dithiazoles, Eur. J. Med. Chem. 33 (1998) 149–153.

[47] J.E. Moore, Certain 4-Halo-5-aryl-1,2,3-dithiazole compounds and their preparation, US Pat. 4059590 (1977).